JOURNAL OF SOLID STATE CHEMISTRY 56, 370–378 (1985)

Vanadyl Hydrogenphosphate Hydrates: $VO(HPO_4) \cdot 4H_2O$ and $VO(HPO_4) \cdot 0.5H_2O$

M. E. LEONOWICZ, JACK W. JOHNSON, J. F. BRODY, H. F. SHANNON, JR., AND J. M. NEWSAM

Exxon Research and Engineering Company, Annandale, New Jersey 08801

Received June 18, 1984

Two vanadyl(IV) monohydrogenphosphate hydrates have been crystallized from aqueous media and their structures determined by single-crystal X-ray diffraction. The first, a tetrahydrate, $VO(HPO_4) \cdot 4H_2O$, is triclinic, $P\bar{1}$, with $a = 6.379(2)$, $b = 8.921(2)$, $c = 13.462(3)$ Å, $\alpha = 79.95(2)$, $\beta = 76.33(3)$, $\gamma = 71.03(3)°$. Final residuals of $R_1 = 0.058$ and $R_2 = 0.065$ were obtained using 1250 unique data and 140 parameters. The second was found to be the hemihydrate, $VO(HPO_4) \cdot 0.5H_2O$, with orthorhombic symmetry, *Pmmn*. Complete structure solution and refinement using data from a 2.7×10^5 μm^3 crystal gave atomic parameters in close agreement with those recently reported in a parallel study (C. C. Torardi and J. C. Calabrese, *Inorg. Chem.* **23**, 1308, 1984). Final residuals $R_1 = 0.041$ and $R_2 = 0.042$ were obtained on optimizing the 45 structural variables using 458 observed intensities. The structures of these two hydrates and that of the pyrophosphate, $(VO)_2P_2O_7$, show a close correspondence. The degree of condensation of the vanadyl octahedra and phosphate tetrahedra, and the amount of water of crystallization in these materials are closely coupled and depend on the formation temperature.

Introduction

The diverse solid-state chemistry of the vanadium phosphates derives both from the accessibility of more than one vanadium oxidation state and from the variety of ways in which phosphate tetrahedra and vanadyl octahedra can be interlinked. Vanadium(V) phosphate, $VOPO_4 \cdot 2H_2O$, for example, undergoes intercalation reactions of two distinct types. During coordination reactions, donor ligands such as pyridine bind directly to V^{5+} centers within the $VOPO_4$ layers, causing the layer spacing to expand and water molecules to be eliminated (*1*). Redox reactions occur when a fraction of the V^{5+} within the layers is reduced to V^{4+} during the intercalation process, requiring that charge-compensating cations be inserted into the water-containing interlayer region (*2*). Structurally, of the vanadium(V) phosphates, $VOPO_4$ (*3–5*) and its dihydrate (*6, 7*) have been studied quite extensively. The vanadium(IV) system is less well documented but structural work on the pyrophosphate $(VO)_2P_2O_7$ (*8*), the dihydrogenphosphate $VO(H_2PO_4)_2$ (*9*), and, very recently, the monohydrogenphosphate hemihydrate, $VO(HPO_4) \cdot 0.5H_2O$ (*10, 11*) has been reported. In the present work we describe competing crystallization between this hemihydrate and a tetrahydrate, $VO(HPO_4) \cdot 4H_2O$, whose structure has been

0022-4596/85 $3.00

determined. We also outline briefly our parallel structural characterization of the hemihydrate and we discuss the interrelationships between these two structures and that of $(VO)_2P_2O_7$.

Experimental

Crystal growth. An aqueous vanadium(IV) phosphate solution was prepared following the procedure suggested in a patent (*12*). V_2O_5 (10 g) was refluxed in concentrated HCl (75 ml). Oxalic acid ($C_2H_2O_4 \cdot 2H_2O$, 1.0 g in 7 ml H_2O) was added followed by H_3PO_4 (85%, 8.2 ml). The dark-blue mixture was refluxed for 20 hr and concentrated to ca. 30 ml by distillation. Water (25 ml) was added to the hot, viscous residue forming a deep-blue solution which was allowed to cool to room temperature. A small amount (0.40 g) of microcrystalline solid was recovered by filtration and identified as $VO(HPO_4) \cdot 0.5H_2O$ by powder X-ray diffraction (*11*). The resulting filtrate deposited $VO(HPO_4) \cdot 4H_2O$ upon standing at room temperature open to the atmosphere for 4 months (Found (calcd. for $VO(HPO_4) \cdot 4H_2O$) V—21.57%(21.69), P—13.23%(13.18); ir spectrum (KBr disk): 3525sh, 3395s,br, 2362w, 2340w, 1648m, 1225sh, 1148sh, 1081s, 1058s, 1023s, 989m, 908w, 890m, 626sh, 516m), while evaporation of a separate portion at 70°C deposited small crystals of $VO(HPO_4) \cdot 0.5H_2O$ in a glassy matrix that could be dissolved away with water. Many repetitions of these procedures were performed. Usually microcrystalline $VO(HPO_4) \cdot 4H_2O$ was deposited at room temperature and $VO(HPO_4) \cdot 0.5H_2O$ or glassy material at elevated temperatures. The crystals used for the diffraction analyses were small (Table I) and were separated from microcrystalline material by extensive sorting under the microscope. The results of Torardi and Calabrese (*10*) indicate that larger crystals of the hemihydrate can be grown hydrothermally at elevated temperatures, although the competition between the hydrated phases is clearly different under such rigorous conditions. Attempts to grow single crystals from nonaqueous solutions of vanadium phosphates that were large enough for X-ray diffraction were unsuccessful.

X-Ray data collection and structure determination for $VO(HPO_4) \cdot 4H_2O$. A small blue-green crystal was mounted on a fine glass fiber with epoxy resin and examined on an Enraf-Nonius CAD-4 automated diffractometer using graphite monochromatized Mo$K\bar{\alpha}$ radiation. Twenty-five reflections located in an automatic search were centered and indexed using a triclinic unit cell and intensity data were then collected over a full hemisphere of reciprocal space restricted by the 2θ range 0° to 50°. Other crystallographic data and experimental details are given in Table I.[1]

[1] All calculations were performed using the Enraf-Nonius Structure Determination Package, an integrated set of crystallographic computer programs for PDP 11 Series computers. Integrated intensities I and their associated standard deviations $\sigma(I)$ were derived via the relations $I = S(C - RB)$ and $\sigma(I) = [S^2(C + R^2B) + (kI)^2]^{1/2}$; C is the total count recorded during the scan, $R = 2.0$ is the ratio of the scanning time to the total background B, S is the scan rate, and $K = 0.05$ is a factor introduced to reflect instrument instability. Structure factor amplitudes $|F_0|$ and their estimated standard deviations $\sigma(F_0)$ were computed from these data using the formula $|F_0| = (I/Lp)^{1/2}$ and $\sigma(F_0) = \sigma(I)/2|F_0|Lp$, where L and p are the Lorentz and polarization corrections. Correction for absorption of X-rays was unnecessary because of the small sample size used in the experiment. Three check reflections periodically monitored throughout the experiment displayed no significant variation. The quantity minimized in the least-squares analysis was $\Sigma w(|F_0| - |F_c|)^2$, where $w = \sigma(F_0)^{-2}$ with $\sigma(F_0)$ defined above. The form of the extinction correction applied was $|F_0|(1 + gI_c)^{-1}$ where the parameter g was included in the least-squares refinement (as expected, given the small sizes of both the hemihydrate and tetrahydrate crystals, the magnitude of the correction is very small). The conventional residual R_1 and the weighted residual R_2 were computed in the usual way. A list of observed and calcualted structure factor amplitudes is given in the supplementary material.

TABLE I

CRYSTALLOGRAPHIC DATA FOR $VO(HPO_4) \cdot 4H_2O$ AND $VO(HPO_4) \cdot 0.5H_2O$

Formula	VPO_9H_9	$VPO_{5.5}H_2$
Formula weight	234.98	171.93
Space group	$P\bar{1}$, No. 2	*Pmmn*, No. 59
Z	4	4
Density (calcd. g cm^{-3})	2.23	2.81
μ(mm^{-1}), Mo$K\bar{\alpha}$(λ = 0.71073 Å)	1.75	2.67
Crystal dimensions (μm)	30 × 50 × 150	75 × 75 × 15
Lattice constants: a(Å)	6.379(2)	7.420(1)
b	8.921(2)	9.609(2)
c	13.462(3)	5.6931(7)
α(°)	79.95(2)	
β	76.33(3)	
γ	71.03(3)	
V(Å^3)	700.0(5)	405.9(4)
Data collection conditions		
Scan type	θ–2θ	θ–2θ
Scan speed (deg 2θ min^{-1})	Variable, 2–13	Variable, 0.6–13
Scan range	2θ(Mo$K\alpha_1$) − 1.1° to 2θ(Mo$K\alpha_2$) + 1.1°	2θ(Mo$K\alpha_1$) − 1.1° to 2θ(Mo$K\alpha_2$) + 1.1°
Unique data examined	2698	1378
Unique data observed	1250, $I > 2\sigma(I)$	458, $I > 2\sigma(I)$
Absorption correction	No	No
Refinement: R_1	0.058	0.041
$R_2(w = [\sigma(F)]^{-2})$	0.065	0.042
ESD, unit weight	1.514	0.838
Data/parameters	8.93	10.18
Extinction parameter, g[1]	2.48×10^{-7}	5.18×10^{-7}
No. of variables	140	45

The structure was initially solved in the noncentrosymmetric space group $P1$ using Fourier techniques, and, after location of all 44 nonhydrogen atoms in the unit cell, converted to the centrosymmetric $P\bar{1}$. The statistics of the distribution of intensities lie roughly midway between the theoretical centric and hypercentric cases (*13, 14*) and the selection of $P\bar{1}$ was confirmed during the subsequent analysis. The center of symmetry in the structure relates adjacent double chains (see Fig. 1). As indicated by the intensity statistics, there is indeed an additional approximate center of symmetry within each double chain (Fig. 2).

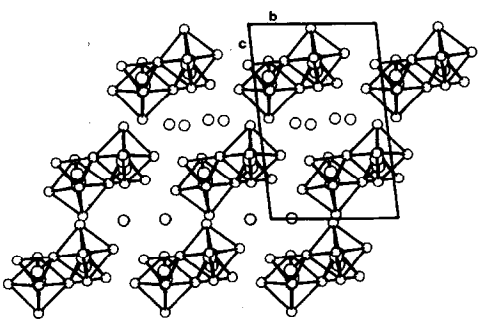

FIG. 1. The double-chain structure of $VO(HPO_4) \cdot 4H_2O$ viewed along the a axis. The waters of crystallization reside in the channels that run parallel to the double chains along a.

In the final cycles of least-squares refinement, anisotropic temperature factors were applied to the vanadium and phosphorus atoms, to the phosphate hydroxyl oxygen atoms, and also to the oxygen atoms of the isolated water molecules. Full anisotropic refinement of the entire structure would have resulted in an unacceptably low data-

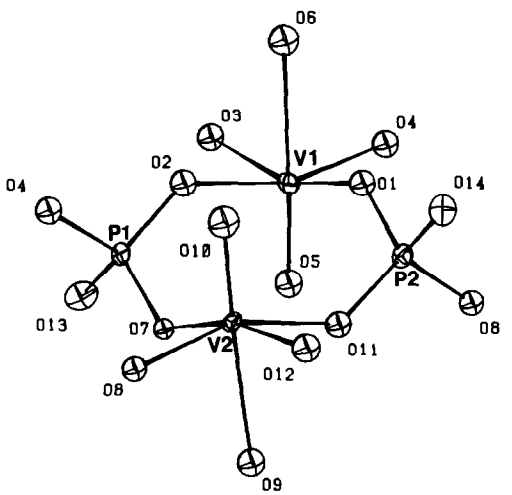

FIG. 2. The structural unit that comprises the double chains in the structure of $VO(HPO_4) \cdot 4H_2O$. An approximate center of inversion relates the separate octahedra and tetrahedra.

to-parameter ratio and, although the selection of which oxygen atoms would be treated anisotropically is somewhat arbitrary, these oxygen atoms were chosen as they appeared most likely to be subject to significant anisotropic vibration. The hydrogen atom positions were not determined. Final structural parameters are given in Tables I–III. Tables VI–VII of the supplementary material[2] list hydrogen bonding O–O contacts, anisotropic thermal parameters, and observed and calculated structure factors. Figures 6 and 7[2] depict the hydrogen bonding.

X-Ray data collection and structure determination for $VO(HPO_4) \cdot 0.5H_2O$. In contrast to the high-temperature synthesis of Ref. (*10*), the ambient pressure crystallizations produced only small particles of the hemihydrate of which the most promising batch was comprised of cylindrical disks of a uniform size (0.075 mm diam. × 0.015 mm thick). Conventional X-ray photographic work did not provide any detectable pattern and hence could not determine whether or not these disks were genuinely single crystals. However, an X-ray rotation picture taken from one of the disks using synchrotron X-radiation had well-defined spots. (The opportunities provided by the brightness of synchrotron X-ray radiation for accessing diffraction data from even smaller crystals has recently been demonstrated (*15, 16*).) The corresponding reflections were all successfully indexed

TABLE II

FINAL POSITIONAL AND ISOTROPIC THERMAL PARAMETERS FOR $VO(HPO_4) \cdot 4H_2O$

Atom	*x*	*y*	*z*	*B*
V1	−0.1575(3)	0.5172(2)	0.8024(1)	0.91(4)+
V2	0.2318(3)	0.8866(2)	0.6911(1)	0.90(4)+
P1	0.3657(4)	0.5128(3)	0.7575(2)	0.83(5)+
P2	−0.2937(4)	0.8903(3)	0.7307(2)	0.96(6)+
O1	−0.283(1)	0.7505(8)	0.8118(6)	1.3(1)
O2	0.139(1)	0.5173(8)	0.8278(5)	1.4(1)
O3	−0.058(1)	0.2732(8)	0.8488(6)	1.4(1)
O4	−0.467(1)	0.4945(8)	0.8243(5)	1.4(1)
O5	−0.089(1)	0.5078(8)	0.6806(6)	1.5(1)
O6	−0.250(1)	0.5153(9)	0.9773(6)	1.8(1)
O7	0.349(1)	0.6557(8)	0.6727(5)	0.8(1)
O8	0.548(1)	0.9014(8)	0.6589(5)	1.2(1)
O9	0.294(1)	0.9228(8)	0.5188(6)	1.5(2)
O10	0.181(1)	0.8765(9)	0.8128(6)	1.9(2)
O11	−0.065(1)	0.8894(8)	0.6633(5)	1.3(1)
O12	0.129(1)	1.1319(9)	0.6704(6)	1.6(1)
O13	0.453(1)	0.3574(8)	0.6981(6)	1.7(2)+
O14	−0.387(1)	1.0404(8)	0.7931(6)	1.5(2)+
O15	0.643(1)	0.1612(9)	−0.0032(7)	2.7(2)+
O16	0.333(1)	0.4029(9)	0.5150(6)	1.8(2)+
O17	0.948(1)	0.2844(9)	0.5084(6)	2.0(2)+
O18	0.189(1)	0.1652(10)	−0.0023(7)	3.1(2)+

Note. The form of the isotropic temperature factor is: $\exp[-B \sin^2 \theta/\lambda^2]$. Equivalent isotropic temperature factors+ for anisotropically refined atoms are derived by the formula: $B_{EQV} = 8\pi^2[\det(U_{ij})]^{1/3}$. Estimated standard deviations in parentheses refer to the last significant digit.

[2] See NAPS Document No. 04242 for 15 pages of supplementary materials from ASIS/NAPS, Microfiche Publications, P.O. Box 3513, Grand Central Station, New York, New York 10163. Remit in advance $4.00 for microfiche copy or for photocopy, $7.75 up to 20 pages plus $.30 for each additional page. All orders must be prepaid.

TABLE III

BOND LENGTHS AND ANGLES IN $VO(HPO_4) \cdot 4H_2O$

V1–O5:	1.605 Å	V2–O10:	1.584 Å
–O6:	2.286	–O9:	2.243
–O3:	2.084	–O12:	2.058
–O1:	1.987	–O7:	1.989
–O2:	2.001	–O11:	2.004
–O4:	1.996	–O8:	2.005
P1–O2:	1.521	P2–O11:	1.526
–O4:	1.506	–O1:	1.503
–O7:	1.550	–O8:	1.524
–O13:	1.595	–O14:	1.578
O5–V1–O6:	176.8°	O10–V2–O9:	175.3°
–O1:	102.5	–O7:	100.0
–O2:	98.7	–O11:	101.6
–O3:	97.9	–O12:	94.5
–O4:	98.2	–O8:	100.7
O6–V1–O1:	80.7	O9–V2–O7:	84.8
–O2:	81.4	–O11:	78.4
–O3:	78.9	–O12:	80.8
–O4:	81.4	–O8:	79.1
O1–V1–O2:	91.1	O7–V2–O11:	88.8
–O4:	91.4	–O8:	90.3
O3–V1–O2:	86.2	O12–V2–O11:	88.8
–O4:	85.2	–O8:	86.4
O1–V1–O3:	159.6	O7–V2–O12:	165.5
O2–V1–O4:	162.0	O11–V2–O8:	157.4
O2–P1–O7:	112.6	O11–P2–O1:	113.6
–O4:	107.7	–O8:	107.0
–O13:	109.1	–O14:	109.5
O7–P1–O4:	114.8	O1–P2–O8:	112.6
–O13:	105.6	–O14:	104.4
O4–P1–O13:	106.6	O8–P2–O14:	109.7
V1–O1–P2:	131.5	V2–O7–P1:	127.6
V1–O2–P1:	133.1	V2–O11–P2:	134.2
V1–O4–P1:	136.0	V2–O8–P2:	130.1

Note. The estimated standard deviation of the bond lengths is 0.007 Å, of the O–V–O bond angles is 0.3°, and of the O–P–O and V–O–P bond angles is 0.4°.

automatically on the basis of an orthorhombic cell that proved identical to that previously used to index the X-ray powder pattern (*11*). This same crystal was then mounted on the Enraf-Nonius CAD-4 diffractometer employing graphite monochromatized Mo$K\bar{\alpha}$ radiation and with the X-ray tube operating at 1600 W. A slow automatic search eventually yielded 25 reflections that were indexed on the orthorhombic cell (the signal : noise ratio of a diffracted signal measured with the counter is much greater than with film, because the latter samples background throughout the complete exposure). A full hemisphere of intensity data was collected over the range $0° < 2\Theta < 80°$ and these data were later averaged to produce a unique orthorhombic set. An R factor computed from the observed structure factor amplitudes of equivalent reflections was 0.032. The crystallographic data for this material are summarized in Table I. The relatively low percentage of reflections adjudged observed at the 2σ level results from the small size of the sample used in the experiment.

The course of the structure analysis was then closely similar to that already described. Despite the small volume of the crystal, the structure was readily solved and, subsequently, the finer structural details were successfully probed. The final atomic parameters given in the tables all agree well with those given in Ref. (*10*). Both of the noncentrosymmetric space groups $Pm2_1n$ and $P2_1mn$ that are consistent with the observed systematic absences,

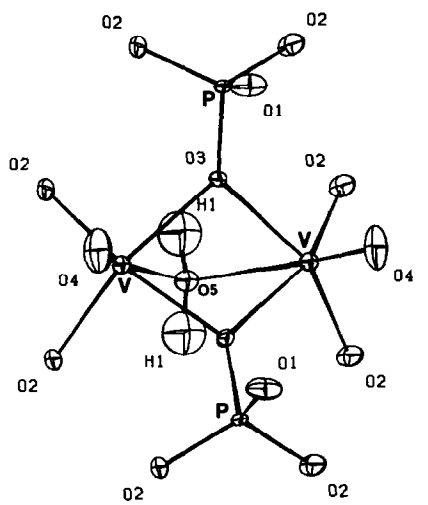

FIG. 3. The structural unit in $VO(HPO_4) \cdot 0.5H_2O$.

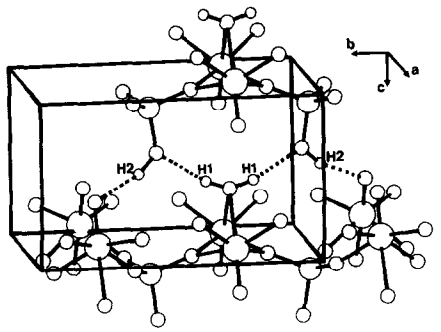

FIG. 4. A section of the $VO(HPO_4) \cdot 0.5H_2O$ structure indicating the hydrogen bonding to the water molecule and the suggested location of the hydroxyl proton, H2.

$hk0$; $h + k = 2n + 1$, were considered in refinement, but the centrosymmetric *Pmmn* was clearly indicated to be the correct choice. The distinction between static and dynamic disorder for O1 and O4 across the mirror planes was less clear cut, and in the tables the latter model is presented (Fig. 3). The final cycles of refinement included the hydrogen atom site of the water molecule (Fig. 4), which had been located in a previous difference Fourier synthesis. The final figures-of-merit, atomic parameters, and selected distances and angles are presented in Tables I, IV, and V. Tables IX and X of the supplementary material[2] list anisotropic thermal parameters and observed and calculated structure factors.

TABLE IV

FRACTIONAL COORDINATES AND EQUIVALENT ISOTROPIC TEMPERATURE FACTORS FOR $VO(HPO_4) \cdot 0.5\ H_2O$

Atom	*x*	*y*	*z*	*B*
V	0.0418(2)[a]	0.250	0.0308(2)	0.87(1)
P	0.250	0.5329(2)	0.2148(3)	0.55(2)
O1	0.250	0.5072(5)	0.4900(9)	1.55(9)
O2	0.0796(5)	0.6062(3)	0.1515(7)	1.45(6)
O3	0.250	0.3842(5)	0.1114(8)	0.86(8)
O4	−0.0591(8)	0.250	0.273(1)	2.4(1)
O5	0.250	0.250	−0.280(1)	1.1(1)
H1[b]	0.250	0.166	0.668	4.0

[a] Estimated standard deviation in parentheses refers to the least significant digit.

[b] Hydrogen atom included but not refined in the least-squares analysis.

TABLE V

SELECTED DISTANCES AND ANGLES IN $VO(HPO_4) \cdot 0.5\ H_2O$

V–V:	3.090(3) Å	P–O1:	1.586(7) Å
V–O2:	1.949(4)	P–O2:	1.491(4)
V–O3:	2.064(3)	P–O3:	1.545(5)
V–O4:	1.572(6)	O1–H1:	1.949(6)
V–O5:	2.350(6)	O5–H1:	0.859(3)
O2–V–O2:	90.3(2)°	O1–P–O2:	108.2(2)°
O3:	91.2(2)	O3:	103.5(3)
O3:	155.2(2)	O2–P–O2:	115.9(3)
O4:	104.4(2)	O3:	110.1(2)
O5:	84.4(2)	V–O3–V:	96.9(2)
O3–V–O3:	77.3(2)	V–O5–V:	82.2(3)
O4:	99.3(2)	V–O2–P:	148.8(3)
O5:	71.1(2)	V–O3–P:	131.5(1)
O4–V–O5:	167.4(3)		

Results

$VO(HPO_4) \cdot 4H_2O$

Single-crystal growth of the vanadyl hydrogen phosphate hydrates at ambient pressure proved difficult. While concentrated aqueous solutions of V^{4+} and phosphate could be readily prepared, crystallization was very slow, and microcrystalline material was the usual result. Crystallization from concentrated aqueous solution at room temperature consistently yielded the tetrahydrate while crystallization through evaporation at higher temperatures (70–100°C) led to the hemihydrate, the two phases being readily distinguished by their X-ray powder diffraction patterns. Consistent with the more rigorous conditions in the sealed-tube experiments, the previous investigators (*10*) did not report formation of species other than the hemihydrate. The tetrahydrate, $VO(HPO_4) \cdot 4H_2O$, is differ-

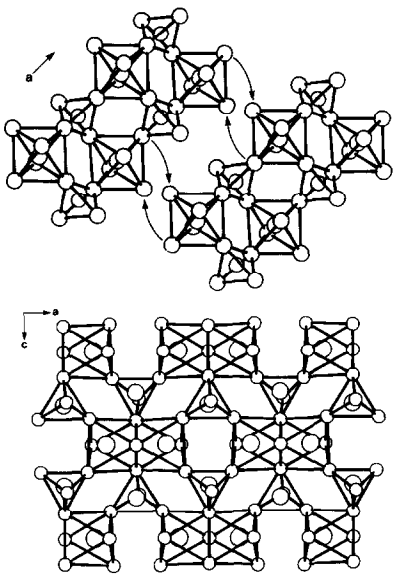

FIG. 5. (a) Two double chains of the $VO(HPO_4) \cdot 4H_2O$ structure depicted as coordination polyhedra viewed in the *ab* plane. The arrows indicate how the chains can be fused by elimination of water to form (b) the $VO(HPO_4) \cdot 0.5H_2O$ structure viewed in the *ab* plane.

ent from a phase of the same formula reported earlier (*17*) as judged both by the published X-ray powder pattern and infrared spectrum. Thermogravimetric analysis of $VO(HPO_4) \cdot 4H_2O$ in flowing He at 10°C/min shows initial loss of two water molecules between 50 and 115°C. As dehydration to the hemihydrate requires loss of 3.5 water molecules, it is possible that other hydrates occur as discrete phases in this system. Above 115°C there is a gradual loss of 2.5 water molecules to give $(VO)_2P_2O_7$ at 500°C. The observed total weight loss of 34.25% agrees with that calculated from the formula (34.50%).

The unit that comprises the framework of the $VO(HPO_4) \cdot 4H_2O$ structure is shown in Fig. 2. The asymmetric unit contains two independent vanadyl octahedra and phosphate tetrahedra sharing oxygen atoms that are related by approximate inversion symmetry. The vanadyl oxygen atoms are O5 and O10. O13 and O14 are the phosphate hydroxyl oxygen atoms. A structural unit analogous to that shown in Fig. 2 is found in $VOSO_4 \cdot 3H_2O$ (*18–20*), but the unit in that structure is isolated, with H_2O molecules in the vanadium coordination positions occupied here by O4 and O8.

In $VO(HPO_4) \cdot 4H_2O$ each vanadyl octahedron shares *trans* oxygen atoms with phosphate tetrahedra so as to form an infinite single chain of alternating octahedra and tetrahedra. Each vanadyl octahedron also shares an oxygen atom with a phosphate tetrahedron in a parallel single chain, thus forming the infinite covalently linked double chain that lies parallel to the crystallographic *a* direction. The double chains are related by lattice translations in the *b* direction, thus forming the rippled sheet of the structure as shown in Fig. 5a. Hydrogen bonds between covalently bonded oxygen atoms of the coordination polyhedra link the double chains together. There are two hydrogen bonds that crosslink the chains in the *b* direction. One links hydroxyl oxygens O13 of the P1 tetrahedra to hydroxyl oxygens O14 of the P2 tetrahedra in the next double chain of the sheet. The other connects O3 of the V1 octahedron to O12 of the V2 octahedron in the adjacent chain. The O–H··O bond lengths are 2.855(8) and 2.740(9) Å, respectively. This type of double chain is also found in $Mo(OH)_3PO_4$ (*21*), where the corresponding lattice repeat distance along the chain (6.319(5) Å) is very close to that found here.

Hydrogen bonds also interconnect the double chains in the $0\bar{1}1$ direction. These bonds link the axially coordinated water molecule (i.e., O6 or O9, the oxygen atoms *trans* to those oxygen atoms with short V–O bond lengths) of each vanadyl octahedron to two oxygen atoms of a phosphate tetrahedron in the adjacent double chain. The hydrogen bond distances are O6–O2, 2.82(1) Å; O6–O4, 2.86(1) Å; O9–O8, 2.789(9) Å; and O9–O11, 3.101(9) Å. This

hydrogen bonding network between the double chains forms channels running parallel to the *a* axis that house the isolated water molecules (Fig. 1). Oxygen atoms O15 and O18 lie within the channel that passes through the origin of the unit cell, while O16 and O17 are contained in the channel that passes through the center of the cell. There are a number of distances between these atoms and other atoms in the structure which are in the range of normal hydrogen bond lengths. All distances less than 3.1 Å are given in Table VI of the supplementary material, together with Figs. 6 and 7 which show the hydrogen bonding in more detail.

$VO(HPO_4) \cdot 0.5H_2O$

The framework of the hemihydrate has been described in some detail (*10*). The pairs of face-sharing vanadium(IV) octahedra found in this structure also make up the primary structural unit in $Cs_3V_2O_2F_7$ where the three fluorine atoms define the shared face (*22*). The corresponding V–V separation (2.995(7) Å) is similar to that observed here, 3.090(3) Å. The separate sheets of interlinked vanadyl octahedra and phosphate tetrahedra are held together by a tight network of hydrogen bonds. The protons (H1) of the shared water molecule O5 are directed toward the hydroxyl oxygen atoms O1, 2.8 Å away in the adjacent layer. The position of the remaining hydroxyl proton was not determined from diffraction data, but interactive computer modeling (*23*) of the local structure indicates its probable location (Fig. 4). The O1–H··O4 hydrogen bond distance shown is 3.045 Å. The approximately tetrahedral coordination of the water molecule, covalently bound to two vanadium atoms and hydrogen bonded to two P–OH groups, explains the high temperature (250–400°C) required to dehydrate this material to $(VO)_2P_2O_7$ and, fortuitously, its accessibility by hydrothermal methods at elevated temperatures (*10*).

Discussion

The structure of $VO(HPO_4) \cdot 0.5H_2O$ can be readily compared to that of $(VO)_2P_2O_7$ (*8*). In the pyrophosphate, the planar arrangement is the same except that the octahedra share only an edge. The layers in $(VO)_2P_2O_7$ are connected by V=O—V and P—O—P bonds in the axial direction rather than through hydrogen bonds between the V—OH_2 and P—OH groups. The similarity of the two structures suggests that the dehydration could proceed topotactically, as has been demonstrated by further studies using kinetic measurements and transmission electron microscopy (*10, 24*). Another compound with a structure similar to that of $VO(HPO_4) \cdot 0.5H_2O$ is $ZnMoO_4 \cdot 2H_2O$ (*25*). In this structure, MoO_4^{2-} tetrahedra take the place of the HPO_4^{2-} groups and $Zn(H_2O)_2^{2+}$ takes the place of $VO(H_2O)^{2+}$ to form octahedra that share edges rather than faces.

The structures of vanadyl hydrogen phosphate tetrahydrate and hemihydrate are also closely related. The coordination geometry around both vanadium and phosphorus is similar in the two structures. Each phosphate group contains three oxygen atoms shared with a vanadium octahedron and an unshared hydroxyl group. The vanadium atoms are coordinated in a C_{4v} distorted octahedral environment with an axial V—O group of bond length ~1.6 Å *trans* to a coordinated water molecule. The four equatorial oxygens are at ~2.0 Å and come from four different phosphate groups in the hemihydrate and from three phosphate groups and a water molecule in the tetrahydrate. Conceptually, the tetrahydrate can be converted to the hemihydrate by removing an equatorial water molecule from each vanadium (O3 and O12 in Fig. 2) and sliding the double chains together so that O12 of one chain is replaced by O4 of an adjacent chain and O3 of that adjacent chain is replaced by O8 of the orig-

inal chain. This translation is indicated by the arrows in Fig. 5. The resulting shared edge (O4–O8) is perpendicular to the *a* direction of the developing hemihydrate structure. The transformation can then be completed by expelling the two water molecules of crystallization and half of the water molecules *trans* to the vanadyl groups. Inverting the resulting VO_5 square pyramids so that the vanadyl oxygens in the pairs are on the same side then allows the remaining water molecules to complete the common face of the vanadium octahedral pairs in the hemihydrate structure.

Acknowledgment

The authors thank A. J. Jacobson for his interest and encouragement throughout the course of this work.

References

1. J. W. Johnson, A. J. Jacobson, J. F. Brody, and S. M. Rich, *Inorg. Chem.* **21,** 3820 (1982).
2. J. W. Johnson and A. J. Jacobson, *Angew. Chem.* **95,** 442 (1983); *Angew. Chem. Int. Ed. Engl.* **22,** 412 (1983).
3. B. Jordan and C. Calvo, *Canad. J. Chem.* **51,** 2621 (1973).
4. B. D. Jordan and C. Calvo, *Acta Crystallogr. Sect. B* **32,** 2899 (1976).
5. M. Tachez, F. Theobald, and E. Bordes, *J. Solid State Chem.* **40,** 280 (1981).
6. H. R. Tietze, *J. Austr. Chem.* **34,** 2035 (1981).
7. M. Tachez, F. Theobald, J. Bernard, and A. W. Hewat, *Rev. Chim. Miner.* **19,** 291 (1982).
8. Yu. E. Gorbunova and S. A. Linde, *Dokl. Akad. Nauk SSSR* **245,** 584 (1979).
9. S. A. Linde, Yu. E. Gorbunova, A. V. Lavrov, and V. G. Kuznetsov, *Dokl. Akad. Nauk SSSR* **244,** 1411 (1979).
10. C. C. Torardi and J. C. Calabrese, *Inorg. Chem.* **23,** 1308 (1984).
11. J. W. Johnson, D. C. Johnston, A. J. Jacobson, and J. F. Brody, *J. Amer. Chem. Soc.* **106,** 8123 (1984).
12. G. Stefani and P. Fontana, U.S. Patent 4,100,106 (1978).
13. E. R. Howells, D. C. Phillips, and D. Rogers, *Acta Crystallogr.* **3,** 210 (1950).
14. R. Srinivasan and S. Parthsarathy, "Some Statistical Applications in X-Ray Crystallography," p. 49, Pergamon, New York (1976).
15. P. Eisenberger, J. M. Newsam, M. E. Leonowicz, and D. E. W. Vaughan, *Nature (London)* **309,** 45 (1984).
16. R. Bachman, *et al., Angew. Chem. Int. Ed. Engl.* **22,** 1 (1983).
17. V. I. Poloiko and V. I. Teterevkov, *Zh. Neorg. Khim.* **26,** 2972 (1981); *Russ. J. Inorg. Chem.* **26,** 1589 (1981).
18. F. Theobald and J. Galy, *Acta Crystallogr. Sect. B* **29,** 2732 (1973).
19. M. Tachez and F. Theobald, *Acta Crystallogr. Sect. B* **36,** 2873 (1980).
20. M. Tachez, F. Theobald, and A. W. Hewat, *Acta Crystallogr. Sect. B* **38,** 1807 (1982).
21. P. Kierkegaard, *Acta Chem. Scand.* **12,** 1701 (1958).
22. K. Waltersson, *Cryst. Struct. Commun.* **7,** 507 (1978).
23. CHEMGRAF program suite, E. K. Davies, Chemical Crystallography Lab, University of Oxford, 1982.
24. E. Bordes, P. Courtine, and J. W. Johnson, *J. Solid State Chem.* **55,** 270 (1984).
25. J. Y. Lemarouille, O. Bars, and D. Grandjean, *Acta Crystallogr. Sect. B* **36,** 2558 (1980).